Role of viscoelastic stresses in turbulent boundary layer flow of drag-reducing fluid

Shinji Tamano[*a)], Michael D. Graham[**] & Yohei Morinishi [*]
[*]*Graduate School of Engineering, Nagoya Institute of Technology, Nagoya, Aichi, 466-8555, Japan*
[**]*Department of Chemical and Biological Engineering, University of Wisconsin-Madison, Madison, WI 53706-1607, USA*

Summary Direct numerical simulations (DNSs) of a zero-pressure-gradient boundary layer flow of a polymeric fluid have been performed at a wide range of Weissenberg numbers in very large streamwise computational domain in order to examine the role of viscoelastic stresses using the FENE-P model. Additionally, simulations in which the polymer stress was turned off beyond a chosen downstream position were performed.

INTRODUCTION

As reported in a previous review [1], numerous DNS studies of turbulent channel flows of viscoelastic fluids can predict some experimental findings such as steeper gradient of mean velocity profile in wall-units and more suppression of wall-normal turbulence intensity and Reynolds shear stress with the amount of the drag reduction. Recently, Xi & Graham [2] found that in the minimal channel, the instantaneous levels of polymer stretching and drag reduction were anticorrelated in time. Although the dependence of turbulence statistics on the drag reduction ratio in the turbulent boundary layer flow was more complex compared to the turbulent channel flow, quite recent DNS of Tamano *et al*. [3] revealed that what occurs temporally in the minimal channel [2] was similar to what occurred spatially in boundary layer flow. However, the role of viscoelastic stresses in drag-reducing turbulent boundary layer flows still remains unknown.

NUMERICAL METHOD AND CONDITIONS

The governing equations are the continuity, momentum equations for incompressible viscoelastic flow, and the FENE-P constitutive equation for the conformation tensor C_{ij}. The second-order accurate finite difference scheme on a staggered grid is used. The semi-implicit time marching algorithm is used where the diffusion term in the wall-normal direction is treated implicitly with the Crank-Nicolson scheme, and the third-order Runge-Kutta scheme is used for all other terms. The momentum-thickness Reynolds number is $Re_{\theta_0} = 500$, which is based on the free-stream velocity U_e and the momentum-thickness at the inlet plane of the driver part θ_0. The Weissenberg number We based on the relaxation time λ is 25, 50, and 100. The ratio of solvent viscosity to zero shear rate solution viscosity β is 0.9. The maximum extension of the polymer L is 100. The size of the computational domain for the present simulations is equal to $(L_x \times L_y \times L_z) = (800\theta_0 \times 30\theta_0 \times 20\pi\theta_0/3)$ in the streamwise, wall-normal, and spanwise directions, respectively. The grid size is $(N_x \times N_y \times N_z) = (1024 \times 64 \times 64)$. The streamwise computational domain is enlarged by a factor of two compared with our previous DNS [3]. The inlet condition for the flow consists of Newtonian velocity data with no polymer stretching. In this paper, $^-$ represents the time-space (spanwise direction) average. The superscript $^+$ represents the variables normalized by wall variables. Readers would see reference [3] for details.

RESULTS

Figure 1(a) shows the streamwise variation in the drag reduction ratio, $DR(x)$, which is function of the streamwise position x. The drag-reducing effect shifts downstream with the increasing We. The streamwise profile of DR shifts downstream with the increase in the relaxation time. At We = 25 and 50, level of DR displays a decaying oscillation in downstream position. At We = 100, very high drag reduction ratio up to about 80% could be obtained around the outlet

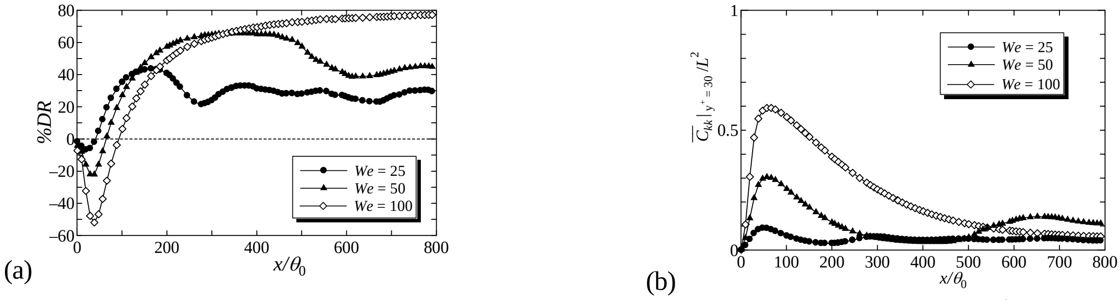

Figure 1. Streamwise variations: (a) drag reduction ratio, (b) trace of conformation tensor at $y^+ = 30$.

---

a) Corresponding author. Email: tamano.shinji@nitech.ac.jp

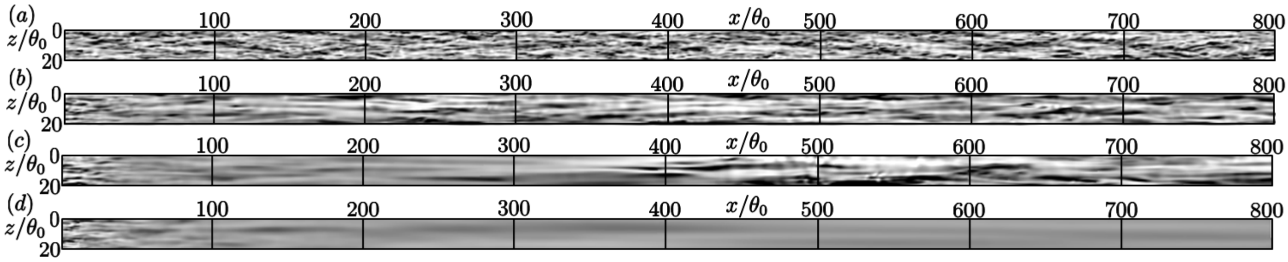

Figure 2. Contour of local wall-shear stress fluctuations ($-0.8 \le \tau''_w / \bar{\tau}^z_w \le 0.8$, white to black): (a) Newtonian, (b) *We* =25, (c) *We* = 50, (d) *We* = 100.

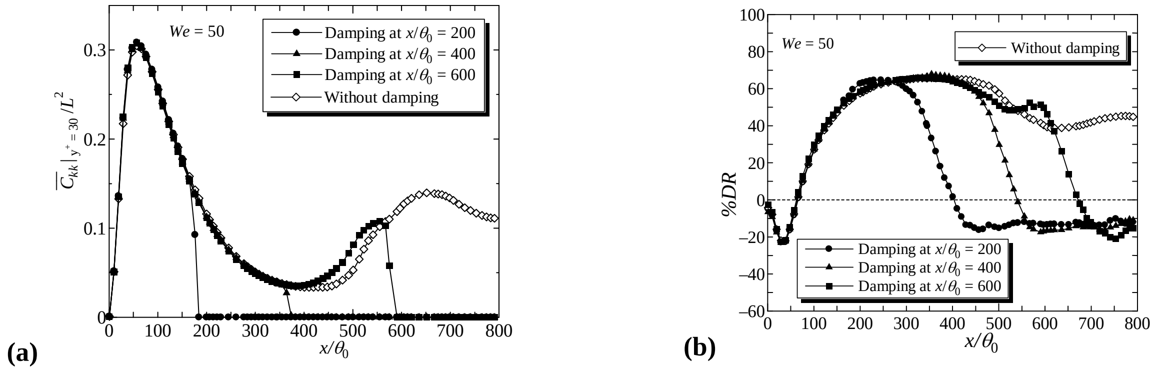

Figure 3. Streamwise variations at *We* = 50 with damping at x/θ_0 = 200, 400, and 600: (a) trace of conformation tensor at y^+ = 30, (b) drag reduction ratio.

plane. Figure 1(b) shows the trace of conformation tensor $\overline{C}_{kk}/L^2$, i.e. the magnitude of polymer elongation at y^+ = 30 is spatially anticorrelated with *DR*. It is worth noting that at *We* = 25 and 50, maxima and minima of *DR* correspond to those of $\overline{C}_{kk}|_{y+=30}/L^2$, respectively.

Figure 2 shows instantaneous contours of local wall-shear stress fluctuation $\tau''_w = \tau_w - \bar{\tau}^z_w$ scaled by the averaged wall-shear stress in the spanwise direction $\bar{\tau}^z_w$. Black and white contours represent high and low wall-shear stress regions, respectively. For the Newtonian fluid, many small high and low wall-shear stress regions appear. On the other hand, at *We* = 25, high and low wall-shear stress regions show larger scales. At *We* = 50, it is interesting that the instantaneous wall-shear stress is almost homogeneous in the upstream region, while some high and low wall-shear stresses appear in the downstream region again. At *We* = 100, the local wall-shear stress is almost uniform except in the upstream region. These observations are consistent with the streamwise variation in *DR* in Fig. 1(a).

To examine the role of the viscoelastic stresses in the downstream evolution of the level of drag reduction, we performed simulations at *We* = 50 in which the viscoelastic stresses were set to zero beyond a fixed downstream distance *b*. Three values of *b* were tested: b/θ_0 = 200, 400, and 600. The removal of the stresses was implemented by multiplying them by the damping function, $W(x) = 0.5 - 0.5 \tanh\{\alpha (x - b)/((1 - 2b)\, x + b)\}/\tanh(\alpha)$, where α is fixed at 50 [see Fig. 3(a)]. Figure 3(b) shows the corresponding streamwise profiles of *DR*. For the cases b/θ_0 = 200 and b/θ_0 = 400, the high level of drag reduction persists for about 100 units downstream of where the polymer stress was turned off, but when b/θ_0 = 600, the level of drag reduction drops immediately. These trends are consistent with results of Xi and Graham [2] in minimal channel flow.

CONCLUSIONS

Direct numerical simulations of a zero-pressure gradient drag-reducing turbulent boundary layer of a viscoelastic fluid were performed using the FENE-P model in very large streamwise computational domain. The role of viscoelastic stresses in drag-reducing turbulent boundary layer flows and the contribution to the drag reduction ratio were discussed.

This work was supported by a Grant-in-Aid for Scientific Research (No. 21760126, No. 23686029) from Japan Society for Promotion of Science.

References

[1] White C.M., Mungal M.G.: Mechanics and prediction of turbulent drag reduction with polymer additives. *Annu. Rev. Fluid Mech.* **40**: 235--256, 2008.

[2] Xi L., Graham, M.D.: Active and hibernating turbulence in minimal channel flow of Newtonian and polymeric fluids. *Phys. Rev. Lett.* **104**: No. 218301, 2010.

[3] Tamano S., Graham M.D., Morinishi Y.: Streamwise variation of turbulent dynamics in boundary layer flow of drag-reducing fluid. *J. Fluid Mech.* **686**: 352--377, 2011.